Spin-exchange frequency shifts in cryogenic and room-temperature hydrogen masers

J. M. V. A. Koelman
Department of Physics, Eindhoven University of Technology, Postbus 513, 5600 MB Eindhoven, The Netherlands

S. B. Crampton
Department of Physics and Astronomy, Williams College, Williamstown, Massachusetts 01267

H. T. C. Stoof
Department of Physics, Eindhoven University of Technology, Postbus 513, 5600 MB Eindhoven, The Netherlands

O. J. Luiten
Natuurkundig Laboratorium, University of Amsterdam, Valckenierstraat 65, 1018 XE Amsterdam

B. J. Verhaar
Department of Physics, Eindhoven University of Technology, Postbus 513, 5600 MB Eindhoven, The Netherlands
(Received 21 March 1988)

We have calculated the spin-exchange shifts of the ground-state $\Delta m_F = 0$ transition of a gas of hydrogen atoms in zero magnetic field from zero temperature up to temperatures of 1000 K. Taking into account the hyperfine interaction during spin-exchange collisions we find shifts nonlinear in the atomic linewidth and not compensated for by the usual methods of tuning the microwave cavities of oscillating hydrogen-maser frequency standards. At room temperatures these shifts affect the H-maser stability at the level of $\delta\omega/\omega \simeq 10^{-15}$. At cryogenic temperatures these shifts are large compared to the potential thermal instabilities of liquid-helium-lined hydrogen masers. A detailed study of these nonlinear shifts reveals several ways to reduce these new sources of frequency instability.

I. INTRODUCTION

The unparalleled frequency stability of the hydrogen maser gives rise to numerous interesting scientific experiments and techniques. Important achievements such as submillisecond-of-arc angular resolutions in radio astronomy[1] and the detection of drifts of the earth's tectonic plates as small as a few centimeters per annum[2] are unthinkable without the very-long-baseline interferometry technique which is founded on the ultrahigh frequency stability of hydrogen masers. Also for physicists the hydrogen maser has developed into an important research tool. State-of-the-art hydrogen-maser instabilities as low as one part in 10^{15} are essential in experiments such as the determination of the Stark shift of the hydrogen hyperfine splitting,[3] and accurate verifications of general relativity theory.[4]

Despite these impressive accomplishments, even more stable frequency standards would be extremely welcome, not only to improve upon the above-mentioned experiments and techniques, but also to open up new horizons in fields as diverse as metrology, physics, astronomy, and geodesy. An illustrative example is the fact that the best atomic clocks available are not sufficiently stable to determine any irregularities in the period of the fastest millisecond pulsar discovered.[5]

As pointed out a decade ago,[6] a cryogenic hydrogen maser might improve considerably upon the frequency stability of a conventional (room-temperature) hydrogen maser, thanks to the reduced thermal noise and cavity pulling at lower temperatures. In 1984 Crampton *et al.*[7] reported maser operation of a solid-Ne-coated hydrogen maser at 10 K. Two years ago Hess *et al.*,[8] Hürlimann *et al.*,[8] and Walsworth *et al.* reported[8] the first observations of maser oscillation with liquid-^{4}He-coated walls at temperatures near 0.5 K. For this type of cryogenic hydrogen maser a frequency instability limit due to thermal fluctuations as low as two parts in 10^{18} was anticipated by Berlinsky and Hardy,[9] leading to the exciting possibility for an improvement in the state of the art of frequency stability with almost 3 orders of magnitude. However, as we pointed out already briefly in a previous publication,[10] one may cast doubt on the realization of that large stability improvement because of frequency instabilities associated with hydrogen-atom spin-exchange collisions.

Spin-exchange collisions between the hydrogen atoms radiating in a hydrogen-maser frequency standard affect the maser frequency in two distinct ways. They directly shift the transition frequency, and they broaden the atomic linewidth, which increases the frequency pulling due to cavity mistuning. The usual theoretical treatment of hydrogen atom spin-exchange collisions,[11] which treats the hyperfine energy levels during the collisions as degenerate, predicts that the direct spin-exchange frequency shifts are proportional to the atomic linewidth, as are frequency shifts due to cavity mistuning.[12] Tuning the cavi-

ty so that the oscillation frequency is independent of atomic linewidth (spin-exchange tuning) is predicted by that treatment to cancel the direct spin-exchange shift against the cavity mistuning shift and hence to leave the oscillation frequency independent of collision rate.[13] As the collision rate is one of the most difficult parameters to stabilize, such "spin-exchange tuning" methods have been important to the development of hydrogen-maser standards.

Including the hyperfine energy-level splitting to first order in a semiclassical spin-exchange collision calculation predicts additional direct frequency shifts not proportional to the total atomic linewidth, but rather proportional to the collision part of the linewidth.[14] This leaves the spin-exchange tuned oscillation frequency independent of collision rate but offset by an amount proportional to that part of the atomic linewidth not caused by collisions.[14] Measurements of this offset in a room-temperature hydrogen maser agreed within errors with the semiclassical estimate of the effect.[14] The offset predicted by that calculation does not adversely affect the stability of hydrogen-maser standards unless something happens to affect that part of the linewidth not due to collisions, such as a change of relaxation by motion of the atoms through magnetic field gradients or a change of relaxation due to interactions with the storage surface.

We have recently done a fully quantum-mechanical calculation of the direct shifts for cryogenic temperatures taking into account the nonzero hyperfine energy-level splitting.[10] We found new effects which are nonlinear in the collision rate and so produce not only an offset of the spin-exchange tuned oscillation frequency, but also a variation of the oscillation frequency with collision rate even after spin-exchange tuning.

In this paper we present a more complete description of the formalism. In addition, we extend the results for the additional direct shifts to a much larger temperature interval so that their implications for hydrogen-maser frequency standards operating at room temperature can be investigated. Near room temperature these additional direct shifts are small, but in contrast to the semiclassical result, are highly nonlinear in the collision rate. We show that the semiclassical approximation used for the calculation of the direct shifts breaks down when the influence of the exchange interaction on the orbital degrees of freedom cannot be neglected. At collision energies large in comparison to the strength of the exchange interaction we show that the quantum-mechanical and semiclassical results agree, in which case both predict direct shifts linear in the collision rate.

A third aim of the present paper is to investigate in detail the variation of the spin-exchange tuned oscillation frequency with collision rate at cryogenic and room temperatures. Although near room temperature the additional direct shifts are small, the variations of the spin-exchange tuned oscillation frequency are large enough to affect the relative stability of the maser at the 10^{-15} level. At cryogenic temperatures variations of the spin-exchange tuned oscillation frequency are orders of magnitude larger than the potential thermal instabilities[9] of liquid-helium-temperature maser standards.

In examining the variation of the spin-exchange tuned frequency with collision rate we are able to propose various strategies to minimize these new sources of frequency instabilities. Several modifications of cryogenic hydrogen-maser designs potentially reduce the dependence of the spin-exchange tuned oscillation frequency on the atomic linewidth by some orders of magnitude, yielding the possibility of cryogenic hydrogen-maser frequency standards with long-term frequency instabilities close to the potential thermal instability limit of 2 parts in 10^{18}.

II. SPIN-EXCHANGE FREQUENCY SHIFTS IN OSCILLATING HYDROGEN MASERS

Our starting point for the derivation of the direct frequency shifts is the evolution equation for the spin-density matrix

$$\frac{d}{dt}\rho_{\kappa\kappa'}+\frac{i}{\hbar}(\varepsilon_\kappa-\varepsilon_{\kappa'})\rho_{\kappa\kappa'}=\dot\rho_{\kappa\kappa'}\mid_{\rm rad}+\dot\rho_{\kappa\kappa'}\mid_0+\dot\rho_{\kappa\kappa'}\mid_c . \tag{1}$$

In this equation ρ is the 4×4 one-particle spin-density matrix in which the Greek subscripts take the values a, b, c, and d, the ground-state hyperfine levels in order of increasing energy ε_α (see Fig. 1). The first term on the right-hand side of Eq. (1) is the radiation term resulting from the interaction of the atomic magnetic moments with the rf cavity magnetic field. The second term on the right-hand side represents all time-independent one-atom terms such as wall collisions, finite cavity residence time, and interactions with magnetic field inhomogeneities.

The third term on the right-hand side of Eq. (1), the collision term, may be derived as follows. We start with a system of N ground-state hydrogen atoms mutually interacting via a central spin-dependent (singlet or triplet) interaction enclosed in a large but finite volume L^3. At the end of this derivation we take the limit $L\to\infty$. The time evolution for the single-particle distribution matrix $F^{(1)}$ can be expressed in terms of the pair-distribution matrix $F^{(2)}$ via the first equation of the quantum-mechanical Bogoliubov-Born-Green-Kirkwood-

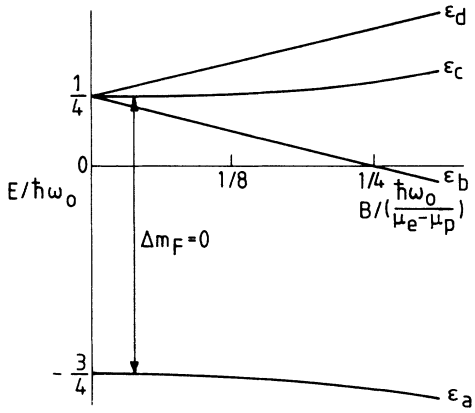

FIG. 1. Atomic hydrogen ground-state energy levels.

Yvon (BBGKY) hierarchy,[15] which in some suitable single-particle basis can be written

$$\frac{\partial}{\partial t}F^{(1)}_{kk'}+\frac{i}{\hbar}\sum_p (H_{kp}F^{(1)}_{pk'}-F^{(1)}_{kp}H_{pk'}) = \frac{-i}{\hbar}\sum_{p,m,n}(V_{kp,mn}F^{(2)}_{mn,k'p}-F^{(2)}_{kp,mn}V_{mn,k'p}) . \quad (2)$$

Here H represents the single-particle Hamiltonian and V the pair interaction. This equation may be converted to a closed equation for the single-particle distribution matrix by expressing the pair matrix at the right-hand side in terms of the single-particle distribution matrix. To first order in the hydrogen-atom density and assuming at times long before a binary collision the absence of any correlation between the atoms not due to particle indistinguishability (molecular chaos assumption), the pair density matrix in Eq. (2) may be written

$$F^{(2)}_{kl,mn}=\sum_{p,q,r,s}\Omega^{(+)}_{kl,pq}(F^{(1)}_{pr}F^{(1)}_{qs}+\epsilon F^{(1)}_{ps}F^{(1)}_{qr})\Omega^{(+)\dagger}_{rs,mn} , \quad (3)$$

in which $\Omega^{(+)}$ is the causal two-body Møller wave operator,[16] while the statistics sign $\epsilon=+1$ for a gas of hydrogen atoms, being (composite) bosons ($\epsilon=-1$ applies to the case of fermions). To be more definite we work in a single-particle basis $\{\,|\,n\,\rangle\}$ in which the single-particle Hamiltonian is diagonal ($H\,|\,n\,\rangle=E^0_n\,|\,n\,\rangle$). Furthermore, we restrict ourselves to spatially homogeneous systems so that these single-particle states are common eigenstates of the momentum operator and the hyperfine spin Hamiltonian, $|\,n\,\rangle=|\,\underline{k}_n,\nu\,\rangle$. We have $E^0_n=\hbar^2\underline{k}_n^2/2m_H+\varepsilon_\nu$, and the single-particle density matrix is diagonal in the momentum indices. Transforming to the interaction representation,

$$\tilde{F}_{kn}=F^{(1)}_{kn}\exp\left[\frac{i}{\hbar}(E^0_k-E^0_n)t\right] ,$$

we find

$$\frac{\partial}{\partial t}\tilde{F}_{kk'}=\frac{-i}{\hbar}\sum_{m,n,p,q,r,s,l}[V_{kl,mn}\Omega^{(+)}_{mn,pq}(\tilde{F}_{pr}\tilde{F}_{qs}+\epsilon\tilde{F}_{ps}\tilde{F}_{qr})\Omega^{(+)\dagger}_{rs,k'l}-\Omega^{(+)}_{kl,pq}(\tilde{F}_{pr}\tilde{F}_{qs}+\epsilon\tilde{F}_{ps}\tilde{F}_{qr})\Omega^{(+)\dagger}_{rs,mn}V_{mn,k'l}]\exp\left[\frac{i}{\hbar}\Delta Et\right] . \quad (4)$$

The "energy inelasticity" $\Delta E\equiv E^0_k-E^0_{k'}+E^0_r-E^0_p+E^0_s-E^0_q$ in the exponent on the right-hand side can only receive a contribution due to the hyperfine energy-level separations since $\tilde{F}$, being diagonal in momentum, does not couple between different kinetic energies. Terms with $\Delta E\neq 0$ average out on time scales long in comparison with the hyperfine precession time scale $\hbar/\Delta E$. So, in the long-time limit, we may restrict the summations on the right-hand side of Eq. (4) to values $E^0_k+E^0_r+E^0_s=E^0_{k'}+E^0_p+E^0_q$ and replace the exponent by unity. Assuming a dominance of either thermalizing collisions with the walls or elastic collisions between the atoms relative to inelastic collisions, the translational degrees of freedom are Boltzmann distributed as

$$\tilde{F}_{mn}=\tilde{F}_{\underline{k}_m\mu,\underline{k}_n\nu}=NP_{m_H}(\underline{k}_m)\delta_{\underline{k}_m,\underline{k}_n}\rho_{\mu\nu}\times\exp[i(\varepsilon_\mu-\varepsilon_\nu)t/\hbar] , \quad (5)$$

with the single-particle spin-density matrix ρ normalized to unity, $\sum_\alpha\rho_{\alpha\alpha}=1$, and $P_m(\underline{k})$ the Boltzmann distribution for free atoms with mass m also normalized to unity, $\sum_n P_m(\underline{k}_n)=1$. Using the identity

$$P_m(\underline{k})P_m(\underline{k}')=P_{2m}(\underline{k}+\underline{k}')P_{m/2}(\tfrac{1}{2}(\underline{k}-\underline{k}'))$$

and center-of-mass momentum conservation we may carry out the summation over the center-of-mass momenta. Taking the limit $N\to\infty$, $L\to\infty$, $N/L^3=n_H=\text{const}$, and after performing the angular integrations, we finally arrive at

$$\dot{\rho}_{\kappa\kappa'}\,|_c=n_H\sum_{\lambda,\mu,\mu',\nu,\nu'}{}'\rho_{\mu\mu'}\rho_{\nu\nu'}[(1+\delta_{\kappa\lambda})(1+\delta_{\kappa'\lambda})(1+\delta_{\mu\nu})(1+\delta_{\mu'\nu'})]^{1/2}\times\sum_l(2l+1)\left\langle\frac{\pi\hbar}{m_Hk}[S^l_{\{\kappa\lambda\}\{\mu\nu\}}(E_k)S^{l*}_{\{\kappa'\lambda\}\{\mu'\nu'\}}(E_k)-\delta_{\{\kappa\lambda\}\{\mu\nu\}}\delta_{\{\kappa'\lambda\}\{\mu'\nu'\}}]\right\rangle . \quad (6)$$

In this equation the prime on the summation sign indicates the subsidiary condition $\varepsilon_\kappa+\varepsilon_{\mu'}+\varepsilon_{\nu'}=\varepsilon_{\kappa'}+\varepsilon_\mu+\varepsilon_\nu$, while Greek subscripts between curly brackets are a short-hand notation for normalized (anti)symmetric two-body spin states,

$$\{\alpha\beta\}\equiv\frac{\alpha\beta+\epsilon(-1)^l\beta\alpha}{\sqrt{2(1+\delta_{\alpha\beta})}} , \quad (7)$$

which for a gas of hydrogen atoms ($\epsilon=+1$) leads to (anti)symmetric spin states for (odd) even angular momentum numbers l. The s-matrix elements, defined for the various angular momentum numbers so as to form a unitary matrix in spin space, are to be evaluated for a common kinetic energy $E_k=\hbar^2k^2/m_H$ in the entrance channels $\{\mu\nu\}$ and $\{\mu'\nu'\}$, and the brackets $\langle\cdots\rangle$ denote thermal averaging over the wave number k. The final result, i.e., the collision contribution to the spin evolution [Eq. (6)], has already been presented in Ref. 10.

We study situations in which the atoms are stimulated to radiate at one specific transition $\alpha\leftrightarrow\beta$. In that case the

only nonvanishing off-diagonal elements of the spin-density matrix are $\rho_{\alpha\beta}$ and $\rho_{\beta\alpha}=\rho^*_{\alpha\beta}$. The one-particle and collision terms in Eq. (1) contributing to the time development of $\rho_{\alpha\beta}$ are of the form

$$\dot{\rho}_{\alpha\beta}|_0=-(\Gamma_0-i\delta\omega_0)\rho_{\alpha\beta}\ , \tag{8}$$

$$\dot{\rho}_{\alpha\beta}|_c = n_H\rho_{\alpha\beta}\sum_\nu \rho_{\nu\nu}\sum_\lambda \sqrt{(1+\delta_{\alpha\lambda})(1+\delta_{\beta\lambda})(1+\delta_{\alpha\nu})(1+\delta_{\beta\nu})}\times G^{\alpha\beta}_{\nu\to\lambda}\ , \tag{9}$$

in which the complex coefficient $\Gamma_0-i\delta\omega_0$ generally depends in a complicated way on the values of the diagonal spin-density matrix elements $\rho_{\nu\nu}$, but is independent of $\rho_{\alpha\beta}$. The complex coefficients $G^{\alpha\beta}_{\nu\to\lambda}$ describe the contribution of collisions in which a ν-state atom makes a transition to the λ state in colliding with an atom which is in a coherent superposition of the α and β states. These ratelike coefficients may be expressed in terms of complex effective "cross-sections" $\sigma^{\alpha\beta}_{\nu\to\lambda}$ using

$$G^{\alpha\beta}_{\nu\to\lambda}=\langle v\sigma^{\alpha\beta}_{\nu\to\lambda}(E_k)\rangle\ , \tag{10}$$

with $v=2\hbar k/m_H$ being the relative collision velocity. In turn these "cross sections" are given in terms of S-matrix elements via

$$\sigma^{\alpha\beta}_{\nu\to\lambda}(E_k)=\frac{\pi}{k^2}\sum_l(2l+1)\times[S^l_{\{\alpha\lambda\}\{\alpha\nu\}}(E_k)S^{l*}_{\{\beta\lambda\}\{\beta\nu\}}(E_k)-\delta_{\lambda\nu}]\ . \tag{11}$$

Upon substituting

$$\rho_{\alpha\beta}(t)=\rho_{\alpha\beta}(0)\exp[i(\varepsilon_\beta-\varepsilon_\alpha)/\hbar+i\delta\omega-\Gamma]t \tag{12}$$

together with Eqs. (8) and (9) in Eq. (1) for $\kappa\kappa'=\alpha\beta$ and neglecting for a moment the radiation term, we find for the direct frequency shift $\delta\omega$ and the atomic linewidth Γ

$$\delta\omega=\delta\omega_0+\delta\omega_c\ , \tag{13}$$

$$\Gamma=\Gamma_0+\Gamma_c\ , \tag{14}$$

in which the direct frequency shift $\delta\omega_c$ and line broadening Γ_c due to spin-exchange collisions are related to the "cross sections" $\sigma^{\alpha\beta}_{\nu\to\lambda}$ via

$$i\,\delta\omega_c-\Gamma_c=n_H\langle v\rangle\sum_\nu\rho_{\nu\nu}\sum_\lambda[(1+\delta_{\alpha\lambda})(1+\delta_{\beta\lambda})\times(1+\delta_{\alpha\nu})(1+\delta_{\beta\nu})]^{1/2}\times\overline{\sigma^{\alpha\beta}_{\nu\to\lambda}}\ . \tag{15}$$

Here we have introduced the modified thermal averaging $\bar{\sigma}\equiv\langle v\sigma\rangle/\langle v\rangle$, with the thermally averaged collision velocity $\langle v\rangle=(16k_BT/\pi m_H)^{1/2}$.

In a hydrogen maser oscillating at low magnetic field on the $\Delta m_F=0$ transition with unperturbed atomic frequency $\omega_0=(\varepsilon_c-\varepsilon_a)/\hbar$ there is only coherence between the a and c states. Substituting $\alpha\beta=ac$ in the preceding expressions we find at zero magnetic field $G^{ac}_{\nu\to\lambda}=\delta_{\nu\lambda}G^{ac}_{\lambda\to\lambda}$ (no contribution from inelastic processes) and $G^{ac}_{b\to b}=G^{ac}_{d\to d}$, yielding

$$\delta\omega_c=n_H\langle v\rangle[(\rho_{cc}-\rho_{aa})\bar{\lambda}_0+(\rho_{cc}+\rho_{aa})\bar{\lambda}_1+\bar{\lambda}_2]\ , \tag{16}$$

$$\Gamma_c=n_H\langle v\rangle[(\rho_{cc}-\rho_{aa})\bar{\sigma}_0+(\rho_{cc}+\rho_{aa})\bar{\sigma}_1+\bar{\sigma}_2]\ , \tag{17}$$

with the real spin-exchange shift and broadening "cross sections" λ_i and σ_i defined in terms of the $\sigma^{ac}_{\nu\to\nu}$ coefficients by

$$i\lambda_0-\sigma_0\equiv\sigma^{ac}_{c\to c}-\sigma^{ac}_{a\to a}\ , \tag{18}$$

$$i\lambda_1-\sigma_1\equiv\sigma^{ac}_{c\to c}+\sigma^{ac}_{a\to a}-\sigma^{ac}_{d\to d}\ , \tag{19}$$

$$i\lambda_2-\sigma_2\equiv\sigma^{ac}_{d\to d}\ . \tag{20}$$

The elastic S-matrix elements occurring in the expressions for $\sigma^{ac}_{\nu\to\nu}$ follow from the Schrödinger equation describing H + H scattering with an effective central two-body interaction consisting of singlet and triplet potentials,

$$\langle\{\alpha\beta\}|V^c(r)|\{\lambda\delta\}\rangle\equiv\sum_{S=0,1}\langle\{\alpha\beta\}|P_S|\{\lambda\delta\}\rangle V_S(r)\ , \tag{21}$$

with V_0 (V_1) being the single (triplet) potential and P_S standing for the projection operator on the subspace with total electron spin S. Since these projection operators are nondiagonal in the $|\{\alpha\beta\}\rangle$ basis we have to deal with sets of coupled radial equations describing the H + H scattering wave function in the various channels. Calculations of this kind are easily carried out[17] at the low temperature of 0.5 K, where the liquid-^{4}He-covered cryogenic hydrogen maser is to operate: S-matrix elements need to be calculated only at a relatively small number of energy values. For calculations at higher temperatures, such as those necessary to obtain thermally averaged frequency-shift cross sections for room temperature hydrogen masers, however, a coupled-channel approach becomes a tedious task. Fortunately, in this regime it is possible to circumvent this task by means of the degenerate-internal-states (DIS) approximation which neglects the internal energy-level separation and replaces the various internal energy levels ε_α by a common constant ε_0, in which case the equations can be decoupled in transforming to a basis in which the total electron spin S is a good quantum number. Splitting off factors containing the low-energy behavior leads to the result[18,17]

$$\frac{S^{l(\mathrm{DIS})}_{\{\gamma\delta\}\{\alpha\beta\}}(E-\varepsilon_\alpha-\varepsilon_\beta)-\delta_{\{\gamma\delta\}\{\alpha\beta\}}}{(\sqrt{E-\varepsilon_\gamma-\varepsilon_\delta}\sqrt{E-\varepsilon_\alpha-\varepsilon_\beta})^{l+1/2}} = \sum_{S=0,1}\frac{e^{2i\delta^l_S(E-2\varepsilon_0)}-1}{(E-2\varepsilon_0)^{l+1/2}}\langle\{\gamma\delta\}|P_S|\{\alpha\beta\}\rangle\ . \tag{22}$$

Notice that we have some freedom in choosing a value for ε_0. When dealing with elastic S-matrix elements $S_{\{\alpha\beta\}\{\alpha\beta\}}$ a suitable choice is to set $2\varepsilon_0$ equal to the inter-

nal energy in the specific channel under consideration ($2\varepsilon_0=\varepsilon_\alpha+\varepsilon_\beta$), which leads to the evaluation of singlet or triplet phase shifts at an energy equal to the kinetic energy in the elastic channel considered. Substituting expression (22) with this choice of ε_0 for the elastic S-matrix elements in the $\sigma^{ac}_{\nu\to\nu}$ coefficients on the right-hand side of Eqs. (18)–(20) yields

$$\lambda_0^{(\mathrm{DIS})}=\frac{\pi}{2k^2}\sum_{l\ \mathrm{even}}(2l+1)\sin(2\delta_1^l-2\delta_0^l)\ , \tag{23}$$

$$\lambda_1^{(\mathrm{DIS})}=\lambda_2^{(\mathrm{DIS})}=0\ , \tag{24}$$

$$\sigma_0^{(\mathrm{DIS})}=0\ , \tag{25}$$

$$\sigma_1^{(\mathrm{DIS})}=\frac{\pi}{k^2}\sum_{l}(-1)^l(2l+1)\sin^2(\delta_0^l-\delta_1^l)\ , \tag{26}$$

$$\sigma_2^{(\mathrm{DIS})}=\frac{\pi}{k^2}\sum_{l\ \mathrm{odd}}(2l+1)\sin^2(\delta_0^l-\delta_1^l)\ , \tag{27}$$

in which the phase shifts δ_S^l are to be evaluated at a collision energy $E_k=\hbar^2k^2/m_H$. These equations are in agreement with the results obtained by Balling *et al.*

On the basis of previous experience[18,17] one might expect that treating the hyperfine energy levels during collisions as degenerate yields a very accurate description of hydrogen atom spin-exchange collision processes down to zero collision energy, so that the direct frequency shift due to spin-exchange collisions is accurately described by the well-known DIS result

$$\delta\omega_c^{(\mathrm{DIS})}=n_H\langle v\rangle\bar{\lambda}_0^{(\mathrm{DIS})}(\rho_{cc}-\rho_{aa})\ , \tag{28}$$

rendering the more complicated Eq. (16) of less interest. However, as pointed out previously,[10] although $\bar{\lambda}_1$ and $\bar{\lambda}_2$ are indeed small compared to $\bar{\lambda}_0$, in a H-maser $\bar{\lambda}_1(\rho_{cc}+\rho_{aa})$ and $\bar{\lambda}_2$ may be large compared to $\bar{\lambda}_0(\rho_{cc}-\rho_{aa})$. The reason for this is that in having self-sustained maser oscillation $\rho_{cc}-\rho_{aa}$ is strongly reduced by transfer of energy to the cavity electromagnetic field, yielding a strongly suppressed DIS direct frequency shift. Moreover, retaining the radiation term in Eq. (1) for $\kappa\kappa'=ac$ shows $n_H(\rho_{cc}-\rho_{aa})$ to be proportional to the total atomic linewidth[12]

$$n_H(\rho_{cc}-\rho_{aa})=\gamma(1+\Delta^2)\Gamma\ , \tag{29}$$

in which γ is a constant dependent on cavity parameters and Δ is twice the ratio of cavity mistuning to cavity resonance linewidth. This yields the possibility to compensate the DIS direct shifts against shifts due to cavity mistuning.[13] These considerations make it necessary to take into account hyperfine-induced effects in the calculation of the direct frequency shifts. On the other hand, in the equation describing spin-exchange line broadening [Eq. (17)], only the terms having a nonvanishing DIS contribution have to be retained. This is because even when the hyperfine-induced cross section $\bar{\sigma}_0$ is comparable in magnitude to $\bar{\sigma}_1$, the quantity $(\rho_{cc}-\rho_{aa})\bar{\sigma}_0$ can still be neglected compared to $(\rho_{cc}+\rho_{aa})\bar{\sigma}_1$ because $|\rho_{cc}-\rho_{aa}|\ll 1$.

The shift $\Delta\omega$ in the maser frequency is the sum of the direct shift $\delta\omega$ and the shift $\Gamma\Delta$ due to cavity mistuning.[12] In view of the previous paragraph the direct shift due to spin-exchange collisions is calculated using expression (16) with the result (29) substituted and Eq. (17) with $\rho_{cc}-\rho_{aa}=0$ substituted. For later use it is convenient to split the oscillation frequency shift $\Delta\omega$ as a sum of a shift $\Delta\omega_0$ independent of collision rate and a shift $\Delta\omega_c$ vanishing at zero-collision rate,

$$\Delta\omega=\Delta\omega_0+\Delta\omega_c=(\delta\omega_0+\tilde{\Omega}\Gamma_0)+(\tilde{\Omega}-\Omega)\Gamma_c\ , \tag{30}$$

with the dimensionless parameters Ω and $\tilde{\Omega}$ defined as

$$\Omega\equiv-\frac{\bar{\lambda}_1(\rho_{cc}+\rho_{aa})+\bar{\lambda}_2}{\bar{\sigma}_1(\rho_{cc}+\rho_{aa})+\bar{\sigma}_2}\ , \tag{31}$$

$$\tilde{\Omega}\equiv\Delta+\gamma\langle v\rangle\bar{\lambda}_0(1+\Delta^2)\ . \tag{32}$$

Here $\delta\omega_0$ is the direct frequency shift due to one atom processes which in most cases is dominated by the shift due to wall collisions. The combined effect of the shift due to cavity pulling and the direct shift due to almost-pure spin-exchange collisions on the H-maser frequency is described by the parameter $\tilde{\Omega}$. The parameter Ω is a measure for the additional effects of hyperfine-induced spin-exchange shifts on the H-maser frequency. The DIS value for Ω vanishes ($\bar{\lambda}_1=\bar{\lambda}_2=0$), in which case spin-exchange tuning the cavity, i.e., setting Δ so as to make $\Delta\omega$ independent of collisional linewidth, yields the frequency shift purely determined by the shifts due to one-atom processes such as wall collisions, $\Delta\omega=\delta\omega_0$. Taking into account the hyperfine level separation in a semiclassical picture[14] yields Ω to be nonzero but independent of $\rho_{cc}+\rho_{aa}$ ($\bar{\lambda}_1=\bar{\sigma}_1=0$). In this case the spin-exchange tuning procedure leads to an oscillation frequency shift being the sum of a shift due to one-atom processes and a shift proportional to the contribution of one-atom processes to the linewidth $\Delta\omega=\delta\omega_0+\Omega\Gamma_0$. According to the preceding analysis Ω is nonzero and depends in a complicated way on collision rate via the collision-rate dependence of the level population sum $\rho_{cc}+\rho_{aa}$, yielding the oscillation frequency shift to depend on the collision rate even after spin-exchange tuning.

III. HYPERFINE-LEVEL POPULATION DYNAMICS

As is evident from Eqs. (30)–(32), the evaluation of the frequency shift $\Delta\omega$ requires knowledge of the value of $\rho_{cc}+\rho_{aa}$. We determine this parameter starting from Eq. (1), but now for the time evolution of the diagonal spin-density matrix elements. We start by investigating the rate of change of $\rho_{cc}+\rho_{aa}$. Using Eq. (6) we find for the collision term on the right-hand side of Eq. (1) at zero magnetic field

$$\begin{aligned}(\dot{\rho}_{cc}+\dot{\rho}_{aa})\,|_c/n_H=2[&(G_{bd\to ac}+G_{bd\to aa}+G_{bd\to cc})\rho_{bb}\rho_{dd}\\&-G_{cc\to bd}\rho_{cc}^2-G_{aa\to bd}\rho_{aa}^2\\&-G_{ac\to bd}(\rho_{aa}\rho_{cc}+|\rho_{ac}|^2)]\ .\end{aligned} \tag{33}$$

Using the unitarity property of the S matrix, the downward spin-exchange relaxation rates are given by[17]

$$G_{\alpha\beta\to\gamma\delta}\equiv\left\langle\frac{2\pi\hbar^2}{m_H k}\sum_l(2l+1)\times|S^l_{\{\gamma\delta\}\{\alpha\beta\}}(E_k)-\delta_{\{\gamma\delta\}\{\alpha\beta\}}|^2\right\rangle . \tag{34}$$

Again using the dominance of thermalizing elastic collisions over inelastic collisions, the upward relaxation rates $G_{\gamma\delta\to\alpha\beta}$ are related to the corresponding downward relaxation rates $G_{\alpha\beta\to\gamma\delta}$ via a Boltzmann factor

$$G_{\gamma\delta\to\alpha\beta}=e^{-(\varepsilon_\gamma+\varepsilon_\delta-\varepsilon_\alpha-\varepsilon_\beta)/k_BT}G_{\alpha\beta\to\gamma\delta} . \tag{35}$$

The level populations ρ_{aa} on the right-hand side of Eq. (33) may be expressed in terms of $\rho_{cc}-\rho_{aa}$, $\rho_{cc}+\rho_{aa}$, and $\rho_{dd}-\rho_{bb}$. Furthermore, we use the fact that in oscillating H masers $\gamma\Gamma/n_H$ is a small parameter (typically $\gamma\simeq10^9$ cm^{-3}s) yielding $|\rho_{cc}-\rho_{aa}|\ll1$ and $|\rho_{ac}|^2\ll1$, so that Eq. (33) can be approximated by

$$(\dot\rho_{cc}+\dot\rho_{aa})|_c/n_H=\tfrac{1}{2}(G_{bd\to}-G_{\to bd})(\rho_{cc}+\rho_{aa})^2+\tfrac{1}{2}G_{bd\to}[1-2(\rho_{cc}+\rho_{aa})-(\rho_{dd}-\rho_{bb})^2] , \tag{36}$$

with

$$G_{bd\to}\equiv G_{bd\to ac}+G_{bd\to aa}+G_{bd\to cc} , \tag{37}$$

$$G_{\to bd}\equiv G_{ac\to bd}+G_{aa\to bd}+G_{cc\to bd} . \tag{38}$$

We now turn to the remaining terms in Eq. (1) contributing to the rate of change of the level population sum $\rho_{cc}+\rho_{aa}$. No contribution comes from the radiation term. The one-body term, however, does contribute. An important contribution to this term arises from atom flow in and out of the maser bulb. Of the many possible other one-body processes that may affect the level populations, we include transitions due to motion through magnetic field gradients both as an example of the complications introduced by additional hyperfine transition processes and as an example of the opportunities to use these processes to diagnose or even "tune out" frequency instabilities. We thus have[19]

$$\dot\rho_{dd}|_0=-\Gamma_b(\rho_{dd}-\rho^0_{dd})-\Gamma_m(\rho_{dd}-\rho_{cc}) , \tag{39}$$

$$\dot\rho_{cc}|_0=-\Gamma_b(\rho_{cc}-\rho^0_{cc})-\Gamma_m(\rho_{cc}-\rho_{bb})-\Gamma_m(\rho_{cc}-\rho_{dd}) , \tag{40}$$

$$\dot\rho_{bb}|_0=-\Gamma_b(\rho_{bb}-\rho^0_{bb})-\Gamma_m(\rho_{bb}-\rho_{cc}) , \tag{41}$$

$$\dot\rho_{aa}|_0=-\Gamma_b(\rho_{aa}-\rho^0_{aa}) , \tag{42}$$

in which Γ_b and Γ_m are the contributions of atom flow and magnetic field gradients to the atomic linewidth Γ and ρ^0_{vv} are the fractional hyperfine level populations of atoms entering the maser bulb.

For stationary oscillation the total rate of change of $\rho_{cc}+\rho_{aa}$ must be zero, which again using $|\rho_{cc}-\rho_{aa}|\ll1$ leads to

$$(G_{bd\to}-G_{\to bd})(\rho_{cc}+\rho_{aa})^2+G_{bd\to}[1-2(\rho_{cc}+\rho_{aa})-(\rho_{dd}-\rho_{bb})^2]-2n_H^{-1}\Gamma_b[(\rho_{cc}+\rho_{aa})-(\rho^0_{cc}+\rho^0_{aa})]-2n_H^{-1}\Gamma_m[2(\rho_{cc}+\rho_{aa})-1]=0 . \tag{43}$$

Using the fact that the difference between the d- and b-level populations is only affected by relaxation due to atom flow and magnetic gradients (not by the interaction with the rf cavity magnetic field nor by spin-exchange collisions), we have

$$\rho_{dd}-\rho_{bb}=(\rho^0_{dd}-\rho^0_{bb})\Gamma_b/(\Gamma_b+\Gamma_m) . \tag{44}$$

Using this result, Eq. (43) reduces to a quadratic equation in the single unknown $\rho_{cc}+\rho_{aa}$. Eliminating n_H^{-1} in favor of Γ_c using Eq. (17) with $(\rho_{cc}-\rho_{aa})\bar\sigma_0\simeq0$ leaves this equation quadratic in $\rho_{cc}+\rho_{aa}$ with the partial relaxation widths entering the coefficients only in the form of their ratios. We conclude that $\rho_{cc}+\rho_{aa}$ (and hence Ω) depends on Γ_b, Γ_m, and Γ_c only in the form of a dependence on two of their ratios, for instance, Γ_c/Γ_b and Γ_m/Γ_b.

The various spin-exchange relaxation rates contributing to $G_{\to bd}$ and $G_{bd\to}$ may be calculated using the DIS expression (22) in Eq. (34). A somewhat cruder approximation,[11] a high-energy version of the DIS approximation, consists of a complete neglect of the difference between the channel energies $\varepsilon_\alpha+\varepsilon_\beta$, $\varepsilon_\gamma+\varepsilon_\delta$, and $2\varepsilon_0$ in Eq. (22) which, when substituted in Eq. (34), yields

$$G_{bd\to ac}=G_{ac\to bd}=\langle v\rangle\bar\sigma^{(\mathrm{DIS})}_2 , \tag{45}$$

$$G_{bd\to aa}=G_{aa\to bd}=G_{bd\to cc}=G_{cc\to bd}=\langle v\rangle(\bar\sigma^{(\mathrm{DIS})}_1+\bar\sigma^{(\mathrm{DIS})}_2)/2 , \tag{46}$$

and

$$G_{bd\to}=G_{\to bd}=\langle v\rangle(\bar\sigma^{(\mathrm{DIS})}_1+2\bar\sigma^{(\mathrm{DIS})}_2) , \tag{47}$$

leading to a vanishing quadratic term in Eq. (43), with the corresponding simple solution

$$\rho_{cc}+\rho_{aa}=\frac{1}{2}\frac{G_{bd\to}[1-(\rho_{dd}-\rho_{bb})^2]+2n_H^{-1}\Gamma_b(\rho^0_{cc}+\rho^0_{aa})+2n_H^{-1}\Gamma_m}{G_{bd\to}+n_H^{-1}\Gamma_b+2n_H^{-1}\Gamma_m} . \tag{48}$$

This high-energy approximation is valid only at collision energies which are large in comparison with the internal energy-level splittings. Since at the operating temperatures of liquid-helium-lined hydrogen masers ($T\simeq0.5$ K) typical collision energies are comparable in magnitude to the internal energy-level splittings $[(\varepsilon_b+\varepsilon_d-\varepsilon_a-\varepsilon_a)/k_B=2\hbar\omega_0/k_B\simeq0.14$ K], the solution of the more complicated Eq. (43) rather than Eq. (48) must in general be used as a closed formula for $\rho_{cc}+\rho_{aa}$.

IV. METHODS OF CALCULATION

As is clear from Secs. II and III, to determine the H-maser frequency shift (Eq. 30) we have to calculate several spin-exchange collision cross sections and relaxation rates. We start with the inelastic processes. Substituting the DIS expression (22) in Eq. (34) we find[17]

$$G_{\alpha\beta\to\gamma\delta}=\sum_l (2l+1)\left\langle \frac{2\pi\hbar}{m_H k}\left[\frac{\sqrt{E_k}\sqrt{E_k+\varepsilon_\alpha+\varepsilon_\beta-\varepsilon_\gamma-\varepsilon_\delta}}{E_k'}\right]^{2l+1}\sin^2[\delta_1^l(E_k')-\delta_0^l(E_k')]\right\rangle \times|\langle\{\alpha\beta\}|P_1-P_0|\{\gamma\delta\}\rangle|^2 , \quad (49)$$

with $E_k'=E_k+\varepsilon_\alpha+\varepsilon_\beta-2\varepsilon_0$. As in Eq. (22), we have some freedom in choosing the value of $2\varepsilon_0$. The evaluation of the relaxation rates amounts to a standard phase-shift calculation for singlet- and triplet-potential scattering. In these and all further calculations we use "state-of-the-art" singlet and triplet potentials,[20] including adiabatic, relativistic, and radiative corrections. Nonadiabatic corrections are taken into account simply by replacing the nuclear mass occurring in the adiabatic equations by the atomic mass m_H.[21,10] Choosing $2\varepsilon_0$ in Eq. (49) halfway between the initial and final channel energies, i.e., $2\varepsilon_0=(\varepsilon_\alpha+\varepsilon_\beta+\varepsilon_\gamma+\varepsilon_\delta)/2$, yields good agreement with coupled-channel[17] results (typical deviations below 1%).

The calculation of elastic processes is somewhat more involved. In particular, the hyperfine-induced spin-exchange frequency shift and broadening "cross sections" (λ_1, λ_2, and σ_0) require the evaluation of elastic S-matrix elements taking into account the hyperfine energy-level separation. This can be done by taking the hyperfine energy-level separation into account as a first-order correction to the DIS approximation,[22,10]

$$S^l_{\{\alpha\beta\}\{\alpha\beta\}}=S^{l(\mathrm{DIS})}_{\{\alpha\beta\}\{\alpha\beta\}}+\Delta S^l_{\{\alpha\beta\}\{\alpha\beta\}} . \quad (50)$$

When choosing $2\varepsilon_0=\varepsilon_\alpha+\varepsilon_\beta$ in Eq. (22) the DIS elastic S-matrix elements reduce to

$$S^{l(\mathrm{DIS})}_{\{\alpha\beta\}\{\alpha\beta\}}(E_k)=\sum_{S=0,1} S_S^l(E_k)\langle\{\alpha\beta\}|P_S|\{\alpha\beta\}\rangle , \quad (51)$$

with

$$S_S^l(E)\equiv e^{2i\delta_S^l(E)} , \quad (52)$$

and the first-order correction takes the form

$$\Delta S^l_{\{\alpha\beta\}\{\alpha\beta\}}(E_k)=\Delta^l(E_k)\sum_{\{\gamma,\delta\}}|\langle\{\alpha\beta\}|P_1-P_0|\{\gamma\delta\}\rangle|^2\times\frac{\varepsilon_\gamma+\varepsilon_\delta-\varepsilon_\alpha-\varepsilon_\beta}{2\hbar\omega_0} , \quad (53)$$

with the dimensionless quantity Δ^l defined by

$$\Delta^l(E_k)\equiv\frac{i}{4}\frac{\omega_0 m_H}{\hbar k}\left[\int_0^{r_0}(u_0^l-u_1^l)^2dr+\tfrac{1}{2}(S_0-S_1)^2W\left[O^l,\frac{\partial}{\partial k}O^l\right]_{r=r_0}\right] . \quad (54)$$

Here $W(\ ,\ )$ is a Wronskian, O^l a Hankel-like free outgoing wave with asymptotic behavior $e^{i(kr-l\pi/2)}$, and the radial singlet (triplet) wave functions u_0^l (u_1^l) are normalized so as to have the outgoing part $-S_S^l O^l$. In a classical picture the first-order correction $\Delta S^l_{\{\alpha\beta\}\{\alpha\beta\}}$ arises due to the finite separation of other hyperfine energy levels ($\varepsilon_\gamma+\varepsilon_\delta$) from the total hyperfine energy $\varepsilon_\alpha+\varepsilon_\beta$ associated with the particular elastic channel under consideration, which is felt when making back and forth transitions to other hyperfine levels during the time that the exchange interaction is active.

Using Eqs. (50)–(53) we find for the hyperfine-induced frequency shift and broadening cross sections

$$\lambda_0=\lambda_0^{(\mathrm{DIS})}-\tfrac{1}{2}(\lambda_1+\lambda_2) , \quad (55)$$

$$\lambda_1=\frac{\pi}{2k^2}\sum_l(2l+1)\mathrm{Im}[\Delta^{l*}(S_1^l-S_0^l)/2+(-1)^l\Delta^{l*}(3S_1^l+S_0^l)/2] , \quad (56)$$

$$\lambda_2=\frac{\pi}{2k^2}\sum_l(2l+1)[1+(-1)^{l+1}]\times\mathrm{Im}[\Delta^{l*}(S_1^l+S_0^l)/2] , \quad (57)$$

$$\sigma_0=\frac{-\pi}{2k^2}\sum_l(2l+1)[1+(-1)^l]\mathrm{Re}(\Delta^{l*}S_1^l) , \quad (58)$$

$$\sigma_1=\sigma_1^{(\mathrm{DIS})}-\tfrac{1}{2}\sigma_0 , \quad (59)$$

$$\sigma_2=\sigma_2^{(\mathrm{DIS})} . \quad (60)$$

Classically speaking, this first-order treatment breaks down when the collision time becomes large compared to the precession frequency associated with the internal energy-level splitting. The collision duration is large at low collision energies and at narrow resonances, occurring in the singlet channel at certain collision energies.[23] We were able to find out about the range of applicability of the first-order approach under various circumstances in comparing the first-order results with results obtained with the coupled-channel analysis. This comparison fully confirmed the preceding classical expectation: the agreement of the first-order approach with the coupled-channel method turned out to be excellent except for the dominating $l=0$ partial wave at the low energies relevant for the cryogenic H maser and at energies and l values at which narrow resonances for singlet scattering occur.

The low-energy deviation for $l=0$ is most prominent at collision energies below $2\hbar\omega_0$, due to the fact that the path in the complex plane which is followed by the elastic

S-matrix element $S^{l=0}_{aa,aa}$ when varying the energy shows a 90° kink at $E=2\varepsilon_a+2\hbar\omega_0$ originating from the threshold in the cc channel felt in the aa channel at this energy. This behavior is absent in the first-order calculation which leads to S-matrix elements which all follow smooth paths in the complex plane.

The deviation at singlet resonances turned out to be most prominent for resonance widths roughly comparable to or smaller than the hyperfine energy-level splitting $2\hbar\omega_0$. The quantity $\Delta^l(E)$ characterizing the hyperfine-induced correction to the elastic S-matrix elements is then no longer small compared to unity, yielding a large overestimation of hyperfine-induced effects. Fortunately, we were able to avoid a time-consuming coupled-channel calculation at narrow resonances by devising a modified zeroth-order approach. This approach is based on the fact that we have some freedom in choosing a value for ε_0 in Eq. (22) so as to make the first-order contribution to the elastic S-matrix elements as small as possible. As is clear intuitively, a good choice for ε_0 at narrow singlet resonances appears to be one which gives the first-order correction to the two-body Hamiltonian

$$V'=\sum_{\{\gamma,\delta\}} |\{\gamma\delta\}\rangle(\varepsilon_\gamma+\varepsilon_\delta-2\varepsilon_0)\langle\{\gamma\delta\}| \tag{61}$$

a vanishing expectation value in singlet spin space. The calculation of the elastic S-matrix elements occurring in the expression for $\sigma^{ac}_{v\to v}$ in zeroth order using this choice for ε_0 leads to the evaluation of singlet or triplet phase shifts at energies shifted from the kinetic energy in the particular elastic channel under consideration [Eq. (22)]. In view of the result that all narrow resonances occur at energies which are large in comparison with the internal energy-level splitting (a typical narrow resonance being the $v=11$, $l=13$ resonance at $E\simeq 276$ K), we may neglect the energy difference $\varepsilon_\alpha+\varepsilon_\beta-2\varepsilon_0$ compared to typical kinetic energies in the denominators of Eq. (22). This leads to an expression for the elastic S-matrix elements of the form of Eq. (51) but with the energy argument of the singlet or triplet S matrix on the right-hand side replaced by $E_k+\varepsilon_\alpha+\varepsilon_\beta-2\varepsilon_0$. Using this expression for the elastic S-matrix elements in the $\sigma^{ac}_{\gamma\to\gamma}$ coefficients on the right-hand sides of Eq. (18)–(20) gives rise to nonvanishing hyperfine-induced frequency shift and broadening cross sections. Comparison with coupled-channel results reveals that at narrow resonances these modified zeroth-order results are almost indistinguishable from the exact results.

It is of interest to compare the semiclassical results for the hyperfine-induced frequency-shift cross sections of Ref. 14 in some detail with our quantum-mechanical results. In the semiclassical straight-line calculation spin-exchange collisions are modeled as spin evolutions under the influence of time-dependent spin interactions originating from the triplet and singlet potentials as the particles move along the undeflected classical trajectories. Defining the singlet (triplet) spin propagators G_0 (G_1) as

$$G_S^{(t_+,t_-)}(b,E)\equiv\exp\left[\frac{-i}{\hbar}\int_{t_-}^{t_+}V_S(b,t)dt\right], \tag{62}$$

with b the impact parameter, and neglecting hyperfine-induced effects we find for the semiclassical (SC) elastic S-matrix elements

$$S^{(\mathrm{DIS,SC})}_{\{\alpha\beta\}\{\alpha\beta\}}(b,E)=\sum_{S=0,1}G^{(+\infty,-\infty)}(b,E)\langle\{\alpha\beta\}|P_S|\{\alpha\beta\}\rangle \tag{63}$$

[cf. Eq. (51)]. The first-order corrections to the elastic S-matrix elements take the form of Eq. (53) with $\Delta^l(E)$ replaced by

$$\Delta(b,E)\equiv\frac{-i}{2}\omega_0\int_{-\infty}^{+\infty}(G_1^{(+\infty,t)}-G_0^{(+\infty,t)})\times(G_1^{(t,-\infty)}-G_0^{(t,-\infty)})dt\ , \tag{64}$$

leading to the semiclassical expression for the hyperfine-induced frequency-shift cross section $\lambda_2(E)$,

$$\lambda_2^{\mathrm{SC}}(E)=\tfrac{1}{4}\int_0^\infty \mathrm{Im}\{\Delta^*(b,E)\times[G_1^{(\infty,-\infty)}(b,E)+G_0^{(\infty,-\infty)}(b,E)]\}2\pi b\,db \tag{65}$$

[cf. Eq. (57)]. The analogous expression for $\lambda_1^{\mathrm{SC}}(E)$ is identical to the right-hand side of Eq. (65) except for the replacement of the plus sign by a minus sign. However, it can be shown that the imaginary part of $\Delta^*G_1^{(\infty,-\infty)}$ is just equal to the imaginary part of $\Delta^*G_0^{(\infty,-\infty)}$, so that λ_1^{SC} vanishes. The origin of this cancellation can be traced back to the neglect of the influence of the exchange interaction on the orbital degrees of freedom: generalizing the preceding calculation scheme so as to take into account the difference between the classical singlet and triplet scattering trajectories would yield nonvanishing values for λ_1^{SC}.[14] This picture is confirmed by the numerical results presented in Sec. V.

V. NUMERICAL RESULTS

We first consider the spin-exchange frequency shift and broadening cross sections. Although the cross sections λ_0, σ_1, and σ_2 have already been calculated by several authors,[24,25] we include them here because these previous values for σ_1 differ quantitatively and qualitatively from our values due to the neglect of hyperfine-induced effects at low collision energies. Also due to the use of improved potentials, our results for λ_0, σ_1, and σ_2 differ at low collision energies from previous results.

In Fig. 2 the frequency and broadening cross sections are given as functions of relative collision energy. A prominent feature of Fig. 2 is the occurrence of cusps in the λ_1, σ_0, and σ_1 cross sections at $E=2\hbar\omega_0=0.14$ K. As discussed in Sec. IV, the origin of this behavior can be traced back to threshold effects in the $l=0$ partial wave. The corresponding cusp in the λ_0 cross section is invisible at the scale of this figure since the main contribution to this cross section comes from the DIS term which behaves smoothly as a function of energy. The λ_2 and σ_2 cross sections vanish at zero collision energy and show no

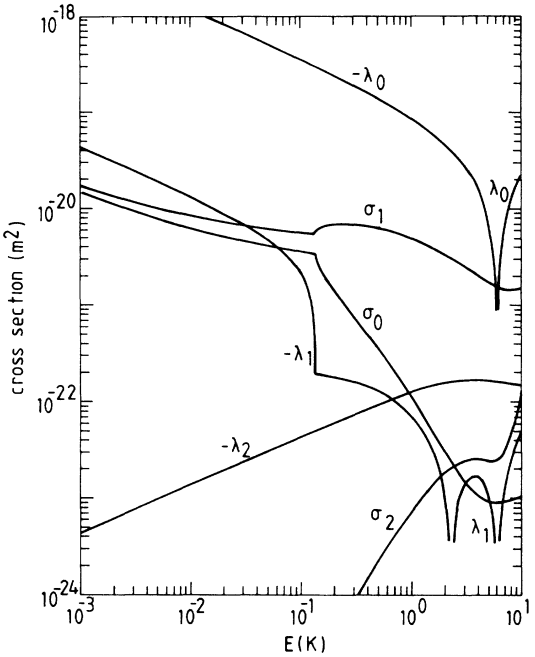

FIG. 2. Spin-exchange frequency shift and broadening cross sections for low collision energies.

cusp behavior as they have no $l=0$ contribution. All other cross sections diverge as $E^{-1/2}$ at low collision energy. For the σ_1 cross section this is in contrast to the finite value at zero collision energy, expected[25] on the basis of DIS considerations.

In Fig. 3 the thermally averaged frequency-shift cross sections are shown as functions of temperature. The low-temperature behavior in this figure corresponds to the low-energy behavior in Fig. 2. The cross section σ_1 is strongly reduced at high temperatures due to a cancellation of contributions from subsequent l values [see Eq. (19)]. Although a semiclassical theory predicts $\bar{\lambda}_1$ to vanish,[14] we find $\bar{\lambda}_1$ to be comparable in magnitude to $\bar{\lambda}_2$, even at temperatures as high as 1000 K. This in contrast to $\bar{\sigma}_1$, which is negligible compared to $\bar{\sigma}_2$ at $T=1000$ K, which by itself would suggest that the semiclassical theory predicting $\bar{\sigma}_1$ to vanish is applicable at this temperature. Calculating λ_1 and λ_2 fully quantum mechanically as well as λ_2 semiclassically assuming straight-line trajectories, we find that λ_1 as well as the difference between the semiclassical and quantum-mechanical values for λ_2 both become small in comparison with λ_2 (Fig. 4) when collision energies become large in comparison with the typical strength of the exchange interaction (a few eV), as may be expected from the picture described above. In this way we arrive at the conclusion that the applicability of the semiclassical straight-line calculation scheme is restricted to collision energies above a few eV (corresponding to temperatures $\simeq 10^5$ K).

To determine the effective spin-exchange relaxation rates $G_{bd\rightarrow}$ and $G_{\rightarrow bd}$ playing a role in the dependence of $\rho_{cc}+\rho_{aa}$ on H-atom density, we have to calculate the DIS values of several spin-exchange relaxation rates $G_{\alpha\beta\rightarrow\gamma\delta}$. In Fig. 5 the rate constants corresponding to the allowed downward spin-exchange transitions at $B=0$ are presented as functions of temperature. Also, the effective rates $G_{bd\rightarrow}$ and $G_{\rightarrow bd}$ are shown. The figure clearly shows that the rate constants involving odd l values only are completely negligible at sub-Kelvin temperatures, but become increasingly important at temperatures above 1 K. Note that the difference $G_{bd\rightarrow}-G_{\rightarrow bd}$, which vanishes in the high-energy approximation, is negligible compared to $G_{bd\rightarrow}$ only at temperatures well above 1 K.

Using the values of $\bar{\lambda}_1$, $\bar{\lambda}_2$, $\bar{\sigma}_1$, and $\bar{\sigma}_2$ displayed in Fig. 3, we are able to determine the dimensionless frequency-offset parameter Ω [Eq. (31)]. Figure 6 shows Ω for two different values of $\rho_{cc}+\rho_{aa}$ as a function of temperature.

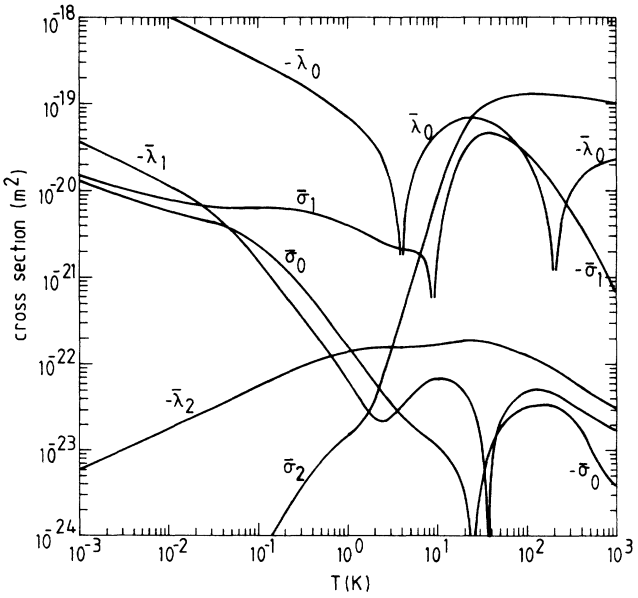

FIG. 3. Thermally averaged values of the frequency shift and broadening cross sections.

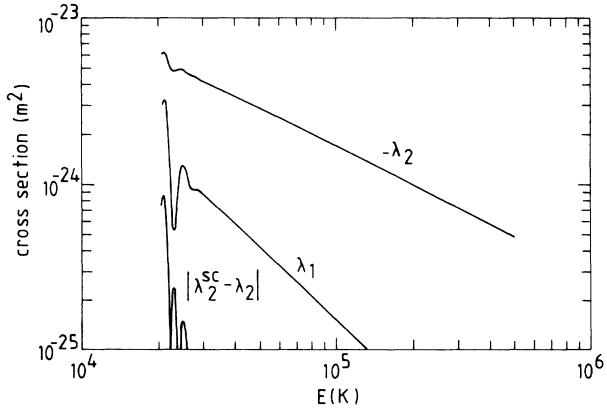

FIG. 4. Values of λ_1 and λ_2 resulting from the quantum-mechanical calculation and the deviation of the semiclassical value for λ_2 with the quantum-mechanical value as functions of energy.

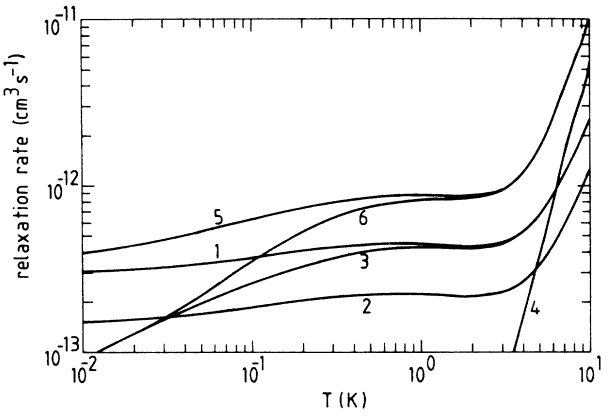

FIG. 5. Degenerate-internal-state values of relaxation rates at $B=0$ for all allowed downward spin-exchange transitions as functions of temperature. 1, $G_{bd\to aa}$; 2, $G_{cc\to aa}$; 3, $G_{cc\to bd}$; 4, $G_{bd\to ac}=G_{cd\to ad}=G_{cb\to ab}$; and the sum rates 5, $G_{bd\to}$; 6, $G_{\to bd}$.

In order to compare this hyperfine-induced frequency-offset parameter with the DIS frequency-offset parameter $\tilde{\Omega}$ we also show the latter as a function of temperature for $\Delta=0$ and a typical value $\gamma=10^9$ cm^{-3} s. Figure 6 shows very clearly that hyperfine-induced spin-exchange frequency shifts become increasingly important at lower temperatures. Both frequency-offset parameters have a finite zero-temperature limit. We find $\Omega(T=0)=3.4$ and $\tilde{\Omega}(T=0,\Lambda=0)$ well below unity but depending on the precise value for γ.

To get an idea whether hyperfine-induced effects lead to important new sources of frequency instabilities we simulated the operation of hydrogen-maser frequency standards at various temperatures. To begin with, we restricted ourselves to the collision-rate-dependent oscillation frequency shift $\Delta\omega_c$ which potentially causes the largest instabilities since the collision rate is difficult to keep constant in an oscillating H maser. Using Eqs. (30)–(32), (43), (44), and the calculated values of the various spin-exchange collision quantities we determined the variations of the oscillation frequency with varying collision rates for various cavity tunings. Since the dependence of Ω on Γ_b, Γ_m, and Γ_c can be written as $\Omega(\Gamma_c/\Gamma_b,\Gamma_m/\Gamma_b)$, Eq. (30) shows that the offset $\Delta\omega_c$ of the oscillation frequency from its value at zero collision rate when expressed in units of Γ_b also depends on the various contributions to the hyperfine relaxation rates as $\Delta\omega_c(\Gamma_c/\Gamma_b,\Gamma_m/\Gamma_b)$. Figure 7 displays $\Delta\omega_c/\Gamma_b$ as a function of Γ_c/Γ_b for a maser operating at 0.5 K with $\Gamma_m=0$ at various cavity frequency settings. As is evident from this figure, the oscillation frequency varies nonlinearly with Γ_c, because of the dependence of Ω on the level populations sum $\rho_{cc}+\rho_{aa}$, which is itself dependent on collision rate. Even when applying the usual "spin-exchange tuning" procedure, i.e., tuning the cavity so that the oscillation frequency is the same at the minimum collision rate at which self-sustained oscillation can be obtained and the maximum collision rate available, there remains an appreciable variation of oscillation frequency inbetween these two values. Because it is difficult to reproduce and keep constant the collision rate in a hydrogen maser, these variations of the "spin-exchange tuned" oscillation frequency with Γ_c pose severe problems to the realization of ultrastable cryogenic hydrogen microwave standards: due to the large slopes present in Fig. 7 variations of the collisional linewidth Γ_c as small as 0.01 s^{-1} lead to variations of the fractional oscillation frequency offset $\Delta\omega/\omega$ of the order 10^{-15}, which is very large when compared to the potential thermal instabilities of cryogenic masers. Of course, when working at very low atom densities the collisional linewidth can be kept stable within a much smaller interval. However, this can only be done at the expense of increasing the oscillation frequency instabilities due to thermal noise.[6,9] In Sec. VI we

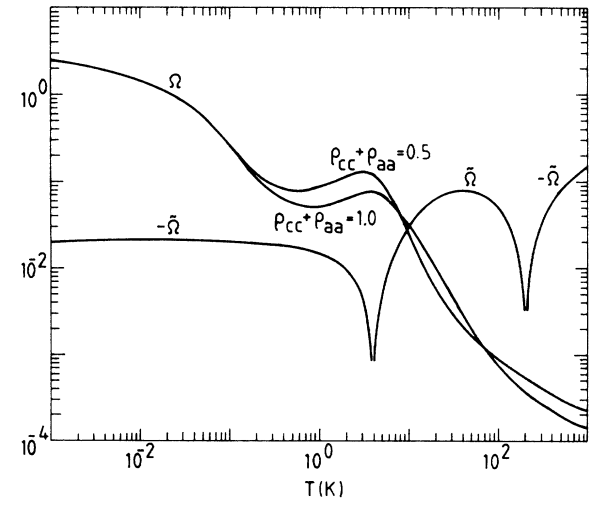

FIG. 6. Dimensionless frequency-shift parameters $\tilde{\Omega}$ (for $\Delta=0$ and $\gamma=10^9$ cm^{-3} s) and Ω (for $\rho_{cc}+\rho_{aa}=0.5,1.0$) as functions of temperature.

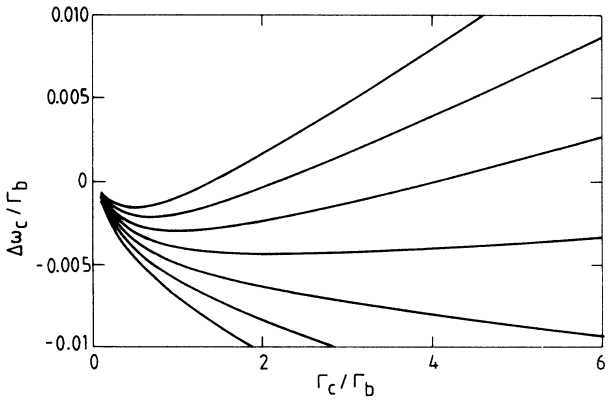

FIG. 7. Variations of fractional frequency offset with collision rate at $T=0.5$ K and $\Gamma_m=0$ for different cavity frequency settings Δ corresponding to $\tilde{\Omega}$ increments of 0.001 between subsequent curves.

investigate strategies which reduce the frequency instability due to variations in the collisional linewidth while leaving the potential thermal instabilities at a level of 2 parts in 10^{18}.

At room temperatures these problems are much less serious. Figure 8 shows the oscillation frequency shifts for various cavity frequency settings as functions of the collisional linewidth for $T=300$ K. The nonlinear variations of oscillation frequency are three orders of magnitude smaller in comparison with the cryogenic results, thanks to the much smaller value of Ω (Fig. 6). When the cavity is tuned so that the oscillation frequency is the same at the minimum and maximum collision rates at which maser oscillation occurs, it leaves a fractional variation of frequency with collision rate typically of order 10^{-15} per Hz of collisional linewidth. In order to keep fractional variations of oscillation frequency due to the nonlinear dependence of linewidth safely below the 10^{-15} level, marking the state of the art of room temperature hydrogen-maser relative frequency instabilities, the variations in collision rate then need only to be kept below the 10% level.

VI. STRATEGIES FOR MINIMIZING THE NONLINEAR DIRECT SHIFTS

Since the instabilities in the maser frequency due to the nonlinear dependence of the oscillation frequency on collision rates seems to be prohibitive in improving substantially upon the stability of room temperature hydrogen masers using cryogenic hydrogen masers, it is necessary to develop techniques for minimizing this nonlinear dependence. We can distinguish three different approaches to accomplish this. First, we may reduce (or even remove) the slope of the cavity frequency as function of collision rate at ambient collision frequency by some refinement of the spin-exchange tuning procedure. Secondly, we can reduce the dependence of the frequency-offset parameter Ω on the level population sum $\rho_{cc}+\rho_{aa}$. As a third possibility we can reduce the dependence of the relative level population sum $\rho_{cc}+\rho_{aa}$ on collision rate.

The first strategy amounts to using a smaller range of Γ_c variations to set the cavity tuning. The optimum spin-exchange tuning procedure clearly would be the one which eliminates the slope of the collision frequency with collision rate at a certain collision rate. However, even the most refined spin-exchange tuning procedure cannot annihilate any nonlinear dependence on collision rate. Indeed, differentiating Eq. (30) twice with respect to the collisional linewidth Γ_c while keeping the linewidth not due to collisions Γ_0 constant yields

$$\frac{\partial^2\Delta\omega}{\partial\Gamma_c^2}=-2\frac{\partial\Omega}{\partial\Gamma_c}-\frac{\partial^2\Omega}{\partial\Gamma_c^2}\Gamma_c\ , \tag{66}$$

which cannot be eliminated by any cavity frequency setting since it is independent of Λ. Using the fact that $\rho_{cc}+\rho_{aa}$, and hence Ω, depends only on the relative magnitudes of the various hyperfine relaxation contributions, it is easily seen that also the dimensionless quantity $\Gamma_c\partial^2\Delta\omega/\partial\Gamma_c^2$ depends only on the ratios of Γ_b, Γ_m, and Γ_c. Figure 9 shows the nonlinearity parameter $\Xi\equiv\Gamma_c\,|\,\partial^2\Delta\omega/\partial\Gamma_c^2\,|$ for $\Gamma_c=\Gamma_b$ at various temperatures with varying Γ_m/Γ_b. A very prominent feature of Fig. 9 is the sharp decrease of the nonlinearity parameter with increasing temperature: at room temperature Ξ is typically 3 orders of magnitude smaller than at $T=0.5$ K. At $T=0.5$ K the parameter Ξ is of the order 2×10^{-3} for the linewidth due to collisions roughly equal to the linewidth due to atom flow and a small contribution of magnetic field gradients to the radiative linewidth. Assuming $\Gamma_c\simeq2\ \mathrm{s}^{-1}$ variations of the collision rate of 1% lead to variations of the fractional oscillation frequency shift $\Delta\omega/\omega$ of approximately 2×10^{-17}, still an order of magnitude larger than the potential thermal instabilities of liquid-helium-lined hydrogen masers. Moreover, it seems unlikely that the optimum spin-exchange tuning procedure can be realized in practice, as such a tuning procedure requires small Γ_c variations to set the cavity

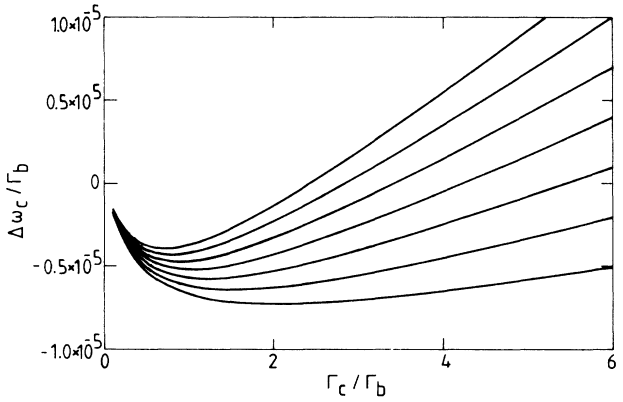

FIG. 8. Variations of fractional frequency offset with collision rate at $T=300$ K and $\Gamma_m=0$ for different cavity frequency settings Δ corresponding to $\tilde{\Omega}$ increments of 0.5×10^{-6} between subsequent curves.

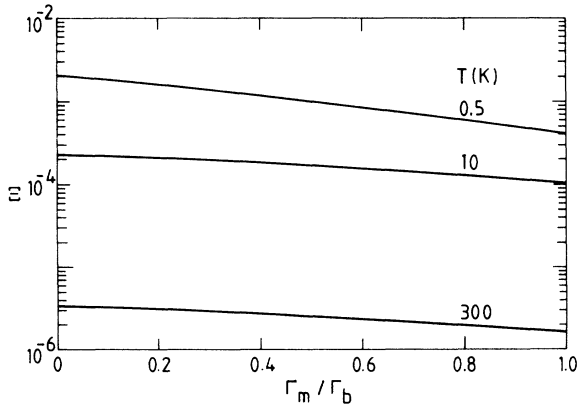

FIG. 9. Nonlinearity parameter Ξ for $\Gamma_c/\Gamma_b=1$ and $T=0.5,10,300$ K as functions of Γ_m/Γ_b.

tuning, which leads to an decrease in the accuracy of the cavity-tuning procedure. In the following we nevertheless make use of the nonlinearity parameter Ξ since it provides a fundamental lower bound to instabilities in the oscillation frequency due to variations in the collision rate.

We have only the temperature as a single adjustable parameter available to reduce the nonlinear direct shifts by the second strategy; reducing the dependence of Ω on $\rho_{cc}+\rho_{aa}$. As is already clear from Fig. 9, higher cryogenic temperatures of about 10 K reduce the nonlinearity parameter roughly by a factor of 10. In this respect neon-surface hydrogen masers operating near 10 K hold some promise although solid neon surfaces are harder to reproduce and maintain than superfluid helium surfaces. The dependence of Ω on $\rho_{cc}+\rho_{aa}$ can be completely eliminated at temperatures at which $\bar{\lambda}_1\bar{\sigma}_2-\bar{\sigma}_1\bar{\lambda}_2$ vanishes. This occurs at very low and very high temperatures, as well as at $T=7.6$ K and $T=77$ K (Fig. 6). From these, the low-temperature limit and the 7.6 K temperature would in principle hold some promise for achieving an ultrastable hydrogen-maser standard because at these temperatures spin-exchange relaxation cross sections are low enough that collisions are not likely to limit the radiated power at achievable hydrogen-atom fluxes. However, the operation temperature of 7.6 K is unsuitable for hydrogen-maser standards as it seems unlikely that any wall coating suitable for operation at this particular temperature exists. Also, the $T\rightarrow 0$ limit is unsuitable not only because of the problem of confining ultracold atoms without disturbing the hyperfine frequency, but also because in this limit the magnitude of Ω exceeds unity, yielding for the cavity mistuning parameter required by the spin-exchange tuning condition $\tilde{\Omega}=\Omega$ a value of order 1, which is unrealistic since the cavity mistuning Δ is limited to values $|\Delta| \ll 1$.

There are several ways to reduce the dependence of the maser frequency on collision rate using the third strategy; reducing the dependence of $\rho_{cc}+\rho_{aa}$ on collision rate. For instance, when working at high atom densities so that $n_H G_{bd\rightarrow} \gg \Gamma_b+\Gamma_m$, Eq. (43) yields a strongly reduced dependence of $\rho_{cc}+\rho_{aa}$ on collision rate. This can be seen clearly in Fig. 10, which shows the nonlinearity parameter for various values of $\Gamma_c/(\Gamma_b+\Gamma_m)$ as functions of $\Gamma_b/(\Gamma_b+\Gamma_m)$: for fixed values of $\Gamma_b/(\Gamma_b+\Gamma_m)$ the nonlinearity parameter decreases sharply with increasing $\Gamma_c/(\Gamma_b+\Gamma_m)$. Another important feature of Fig. 10 is the large dip in the nonlinearity parameter for $\Gamma_b/(\Gamma_b+\Gamma_m)=0.35$. This dip results from the fact that at this value for $\Gamma_b/(\Gamma_b+\Gamma_m)$ for $\rho^0_{dd}-\rho^0_{bb}=\frac{1}{2}$ the level population difference $2(\rho_{dd}-\rho_{bb})=0.35$ [Eq. (44)], which is just equal to the value of

$$\sqrt{(G_{bd\rightarrow}-G_{\rightarrow bd})/G_{bd\rightarrow}}$$

at $T=0.5$ K. Substituting

$$2(\rho_{dd}-\rho_{bb})=\sqrt{(G_{bd\rightarrow}-G_{\rightarrow bd})/G_{bd\rightarrow}}$$

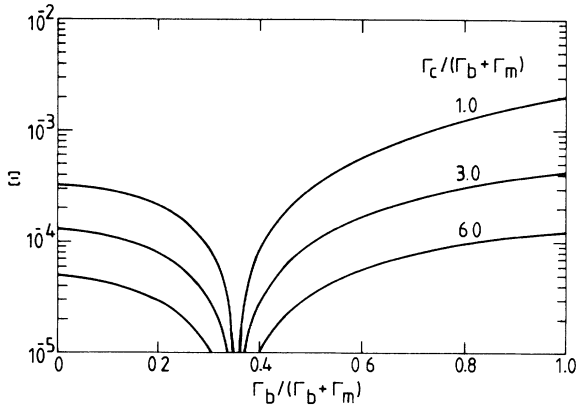

FIG. 10. Nonlinearity parameter Ξ with varying $\Gamma_b/(\Gamma_b+\Gamma_m)$ for various values of $\Gamma_c/(\Gamma_b+\Gamma_m)$ at $T=0.5$ K.

together with $\rho^0_{cc}+\rho^0_{aa}=\frac{1}{2}$ in Eq. (43) yields the level population sum $\rho_{cc}+\rho_{aa}=\frac{1}{2}$ independent of collision rate. This gives rise to a modified tuning procedure which in principle annihilates the collision-rate-dependent oscillation frequency shift $\Delta\omega_c$ completely. The essence of this tuning procedure is first to set the magnetic field inhomogeneities so as to make $\tilde{\Omega}-\Omega$ [Eq. (30)] independent of collision rate before applying the usual spin-exchange tuning procedure. The dependence of $\tilde{\Omega}-\Omega$ on Γ_c can be monitored by determining the oscillation frequency and the total linewidth [which can be determined experimentally from variations $\Delta\omega$ of oscillation frequency with cavity mistuning Δ, as shown by Eqs. (30) and (32)] at three different collision rates: if the oscillation frequency depends nonlinearly on total linewidth at these three points, $\tilde{\Omega}-\Omega$ still has some dependence on collision rate. For $\tilde{\Omega}-\Omega$ independent of collision rate the usual spin-exchange tuning procedure yields $\tilde{\Omega}=\Omega$ and hence a vanishing collision rate dependent shift, $\Delta\omega_c=0$.

Even when $\Delta\omega_c$ is completely removed, we still have to deal with the collision-rate-independent shift $\Delta\omega_0=\delta\omega_0+\tilde{\Omega}\Gamma_0=\delta\omega_0+\Omega\Gamma_0$. For a ^{4}He-lined hydrogen maser operating at a temperature $T=0.5$ K Berlinsky and Hardy predicted[9] that the shift $\delta\omega_0$ could be kept constant against thermal instabilities to within 1 part in 10^{18}. The second term contributing to $\Delta\omega_0$ seems more critical. For $\rho_{cc}+\rho_{aa}=\frac{1}{2}$ and $T=0.5$ K we have $\Omega=0.07$ (Fig. 6). This value implies a maximum allowed instability in the linewidth not due to collisions as low as $\delta\Gamma_0=3.10^{-7}$ s^{-1} in order to achieve a frequency instability of 2 parts in 10^{18}. It seems unlikely that all line-broadening processes contributing to Γ_0 (atom flow, motion through magnetic field gradients, wall collisions, Doppler broadening, etc.) can be kept stable within this limit.

At room temperature $\Omega\simeq 0.0002$, more than two orders of magnitude smaller than at $T=0.5$ K. In order to achieve a frequency instability of 1 part in 10^{15} the linewidth not due to collisions must be kept stable within approximately 0.05 s^{-1}.

ACKNOWLEDGMENT

This work is supported by the National Science Foundation Grant No. PHY-840467, and is part of a research program of the Stichting voor Fundamenteel Onderzoek der Materie (FOM) which is financially supported by the Nederlandse Organisatie voor Wetenschappelijk Onderzoek (NWO).

[1]M. H. Cohen, Proc. IEEE **61**, 1192 (1973).
[2]W. E. Carter, D. S. Robertson, and J. R. Mackay, J. Geophys. Res. **90**, 4577 (1985).
[3]E. N. Fortson, D. Kleppner, and N. F. Ramsey, Phys. Rev. Lett. **13**, 22 (1964).
[4]R. F. C. Vessot *et al.*, Phys. Rev. Lett. **45**, 2081 (1980).
[5]L. A. Rawley, J. H. Taylor, M. M. Davis, and D. W. Allan, Science **238**, 761 (1987).
[6]S. B. Crampton, W. D. Phillips, and D. Kleppner, Bull. Am. Phys. Soc. **23**, 86 (1978); R. F. C. Vessot, M. W. Levine, and E. M. Mattison, in Proceedings of the Ninth Annual Precise Time and Time Interval Conference, 1978 [NASA Technology Report No. 78104, 1978 (unpublished)], p. 549.
[7]S. B. Crampton, K. M. Jones, G. Nunes, and S. P. Souza, in Proceedings of the Sixteenth Annual Precise Time and Time Interval Conference, 1985 [NASA Technology Report No. 8756, 1985 (unpublished)], p. 339.
[8]H. F. Hess, G. P. Kochanski, J. M. Doyle, T. J. Greytak, and D. Kleppner, Phys. Rev. A **34**, 1602 (1986); M. D. Hürlimann, W. N. Hardy, A. J. Berlinsky, and R. W. Cline, *ibid.* **34**, 1605 (1986); R. L. Walsworth, I. F. Silvera, H. P. Godfried, C. C. Agosta, R. F. C. Vessot, and E. M. Mattison, *ibid.* **34**, 2550 (1986).
[9]A. J. Berlinsky and W. N. Hardy, Proceedings of the Thirteenth Annual Precise Time and Time Interval (PTTI) Applications and Planning Meeting, Naval Research Laboratory, Washington, D.C. 1982 [NASA Conference Publication No. 2220, 1982 (unpublished)], p. 547.
[10]B. J. Verhaar, J. M. V. A. Koelman, H. T. C. Stoof, O. J. Luiten, and S. B. Crampton, Phys. Rev. A **35**, 3825 (1987).
[11]L. C. Balling, R. J. Hanson, and F. M. Pipkin, Phys. Rev. **133**, A607 (1964); **135**, AB1 (1964).
[12]S. B. Crampton, Phys. Rev. **158**, 57 (1967).
[13]D. Kleppner, H. C. Berg, S. B. Crampton, N. F. Ramsey, R. F. C. Vessot, H. E. Peters, and J. Vanier, Phys. Rev. **138**, A972 (1965).
[14]S. B. Crampton and H. T. M. Wang, Phys. Rev. A **12**, 1305 (1975).
[15]S. Hess, Z. Naturforsch. **22a**, 1871 (1967).
[16]W. Glöckle, *The Quantum Mechanical Few-Body Problem* (Springer-Verlag, Berlin, 1983).
[17]H. T. C. Stoof, J. M. V. A. Koelman, and B. J. Verhaar, Phys. Rev. B **38**, 4688 (1988).
[18]J. M. V. A. Koelman, H. T. C. Stoof, B. J. Verhaar, and J. T. M. Walraven, Phys. Rev. Lett. **59**, 676 (1987).
[19]D. Kleppner, H. M. Goldenberg, and N. F. Ramsey, Phys. Rev. **126**, 603 (1962).
[20]W. Kolos and L. Wolniewicz, J. Chem. Phys. **43**, 2429 (1965); W. Kolos and L. Wolniewicz, Chem. Phys. Lett. **24**, 457 (1974); J. F. Bukta and W. J. Meath, Mol. Phys. **27**, 1235 (1974); L. Wolniewicz, J. Chem. Phys. **78**, 6173 (1983).
[21]P. R. Bunker, C. J. McLarnon, and R. E. Moss, Mol. Phys. **33**, 425 (1977).
[22]A. M. Schulte and B. J. Verhaar, Nucl. Phys. **A232**, 215 (1974).
[23]T. G. Weach and R. Bernstein, J. Chem. Phys. **46**, 4905 (1967).
[24]A. C. Allison, Phys. Rev. A **5**, 2695 (1972).
[25]A. J. Berlinsky and B. Shizgal, Can. J. Phys. **58**, 881 (1980).